Active damping applied to HSM-driven mechanical loads with elasticity ⋆

Riccardo Antonello, Angelo Cenedese and Roberto Oboe

University of Padova, Department of Management and Engineering, Vicenza, Italy (Tel: +39-0444-998844; (e-mail: riccardo.antonello@gest.unipd.it; angelo.cenedese@unipd.it; roberto.oboe@unipd.it)

Abstract: Hybrid Stepper Motors (HSM), together with the microstepping driving technique, are widely used in many motion control applications, given their low cost and high reliability. On the other hand, being controlled in an open loop fashion, they cannot achieve high levels of performance, this mainly due to the absence of a load-side position sensor. In this paper, we address the problem of controlling the motion of a mechanical load, driven by a HSM, in presence of a flexible mechanical transmission between motor and load. This is a typical industrial scenario, in which the problem of the oscillations arising from the excitation of the mechanical resonance by various disturbances (including torque ripple) is usually addressed by severely limiting the overall dynamic performance. In this paper, we propose the use of an active damping strategy, which allows for the improvement of the dynamic response and an excellent rejection of the oscillations caused by the torque ripple. The proposed technique does not require the re-design of the existing equipments, since it is based on an enhancement of the standard microstepping, in which the angle of the stator flux is properly modulated, to produce a compensating torque and, in turn, damp the oscillatory modes. Such modulation is based on the proper processing of the measurements obtained from a load-side MEMS accelerometer, which can be easily fitted into existing setups. Experimental results confirm the effectiveness of the proposed solution.

Keywords: Hybrid stepper motor, active damping, MEMS accelerometers

1. INTRODUCTION

Hybrid Stepper Motors (HSM) are widely used in many motion control applications, where there are tight cost constraints and it is acceptable to have a limited level of performance. Their structure is composed of a cylindrical permanent magnet, polarized axially, covered by toothed soft steel cores, as shown in Fig. 1. This type of motor works as a stepping motor by the combined principles of the permanent-magnet motor and the variable reluctance motor (Kenjo [1984]). The two cores are angularly displaced by half of a teeth and this, combined with the particular toothed structure of the stator (with the same pitch of the rotor), allows steps with the width of a quarter of a teeth, when the two phases of the stator windings are driven in an on/off fashion (see Fig. 2). HSMs driven in such a way share with all stepper motor the problem of a non-smooth torque generation, together with an oscillatory behavior in step-to-step motion. A widely applied driving technique that partially alleviates the above problems, is the so-called microstepping (Rahman and Grantham [1990]), in which the phase currents are two sinusoids in quadrature (see Fig. 3). With this driving technique, the stator flux rotates smoothly, thus limiting torque ripple and rotor oscillations.

We will discuss later some details on torque generation in HSM, but it is well known (Ahn et al. [2005]) (Bodson et al. [1993]) (Blauch et al. [1993]) that, even with the use of microstepping, torque ripple is not easy to be avoided, especially due to the presence of a large detent torque. This fact has often limited the application of HSM in all those systems in which the presence of mechanical resonances could amplify the effects of torque ripple, resulting in an unacceptable load oscillation. Some authors have proposed the use of complex ripple minimization techniques, but all of them require a rotor position sensor, thus reducing the cost benefit of having an open loop position actuator (Ahn et al. [2005]) (Kos et al. [2006]) (McInroy et al. [1995]).

Vibration suppression and control in mechanical loads with resonant modes is a widely studied subject and several techniques have been proposed, like input shaping and active damping (Miu [1993]). As for input shaping, this refers to a set of techniques aiming at reducing the overall (or residual) energy around the resonance frequency and, in turn, limit the oscillatory behavior. Minimum jerk and reference filtering are usually the simplest methods to avoid the excitation of the resonant modes, while minimum energy control aims at the design of reference trajectories that will end with null energy stored in the resonant element of the controlled system. All the input shaping

⋆ This work has been partially supported by the Programma Operativo F.S.E. 2007-2013 Regione Veneto, Codice Progetto 2105/101/17/2214/2009 ("Modellizzazione Orientata al Controllo di Sistemi Meccatronici").

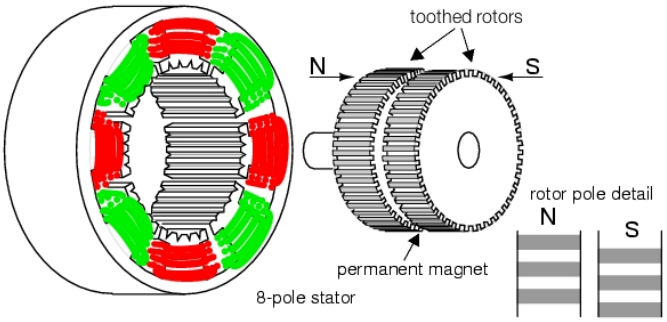

Fig. 1. Hybrid stepper motor.

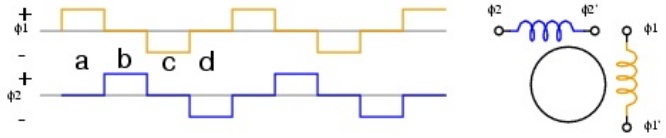

Fig. 2. Square wave driving of 2–phase stepper motor.

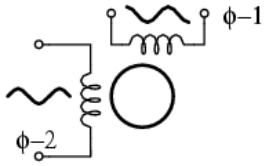

Fig. 3. Microstepping: sinusoidal driving of 2–phase stepper motor.

techniques, however, are best suited for point-to-point motions, and they do not provide any remedy against the load oscillations due to disturbances, like torque ripple, always present in HSMs. Active damping has found a large application in the control of flexible structures, and it has been implemented either by distributing damping actuators along the structure to be controlled (e.g. piezoelectric actuators on the modal nodes of an elastic beam) or, in case a single actuator is available, by properly controlling the generated torque. In principle, the idea is simple: inject a force/torque, equivalent to that produced by a viscous damper, to reduce the amplitude of the vibrations, caused either by disturbances or transients in point–to–point motions. This idea, of course, has a straightforward application in all those systems provided by a torque-controllable actuator (e.g. DC motor, AC brushless motors etc.), but it has never been applied in position controlled actuators, like HSMs.

In this paper we propose the application of an active damping technique to a system with mechanical resonances and driven by a HSM. We will show in the following how it is possible to generate a torque for the compensation of the oscillatory behavior by using a phase modulation of the currents applied to the stator windings. The modulation, in turn, is driven by the velocity of the load, obtained by processing the output of a low-cost MEMS accelerometer. The paper is organized as follows. Section 2 describes the positioning unit for surveillance camera that has been used as a case study for the application of the proposed technique. Section 3 describes the mechanical model of the system to be controlled, with some details on the factors that may lead to plant changes and, in turn to robustness problems. Section 4 describes the control law design, together with the solution adopted to generate the damping torque and the limits on performance posed by the actuator used. The experimental results obtained are reported in Section 5, while conclusions and future research directions are presented in Section 6.

2. CASE STUDY - POSITIONING UNIT FOR SURVEILLANCE CAMERA

In order to test the feasibility of an active vibration suppression scheme, when the load is driven by a HSM, we used a positioning unit for surveillance cameras, shown in Fig. 4. This is a pan–tilt unit, with adjustable focus and zoom. In pan and tilt, the camera is moved by two HSMs, connected to the load through a reduction unit, composed of two gears and a toothed belt (Fig. 5). The positioning unit can be controlled manually, via a user console, or automatically, with a video processing unit that commands the pan and tilt angle in order to track a moving target.

This unit operates outdoor, often facing harsh environmental conditions and it can be mounted on a wide variety of supports, ranging from concrete walls to long (and flexible) supporting poles. Additionally, it is subjected to various disturbances (ranging from wind gusts to birds hanging on the unit) and some of the operating parameters (e.g. friction of the sealing rings, stiffness of the belts, etc.) may widely change with the temperature (the unit must be fully operative from -40 to +60 centigrades). Finally, using an elastic transmission belt, the system presents mechani-

Fig. 4. Positioning unit for surveillance camera.

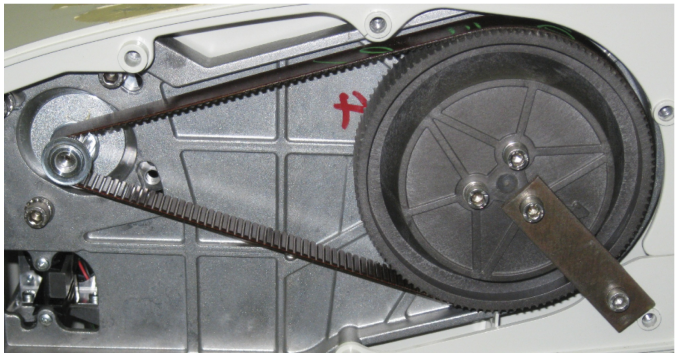

Fig. 5. Reduction unit with gears and toothed belt.

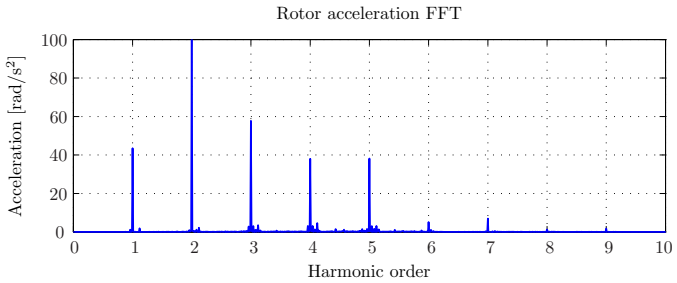

Fig. 6. Torque harmonics of the HSM.

cal resonances, which may amplify the effects of the torque ripple generated by the HSM and other disturbances.

The unit comes without a load position sensor, so the tracking of a moving target is performed simply by acting on the HSM position, without any feedback. Rotations of the unit at a constant angular rate ω_t (e.g. when following a target moving at a constant speed) are obtained with a microstepping drive, i.e. by applying to the stator windings two quadrature sinusoidal currents with a fixed frequency $\omega_u = (N_r/N_G)\,\omega_t$, where N_r is the number of pole pairs of the HSM and N_G is the gear ratio. In such operating conditions, the torque ripple generated by the HSM is composed of several harmonics, with a base frequency equal to that of the stator currents. Such harmonics are generated by both the driving amplifiers (which may introduce differences in offsets and amplitudes of the phase currents) and motor imperfections (Bascetta et al. [2010]). As an example, the HSM used in moving the pan angle of the unit has a measured torque ripple spectrum as in Fig. 6.

3. MECHANICAL SYSTEM MODELING AND IDENTIFICATION

In order to perform the design of the active damping of the vibrational modes for the system described in the previous section, it is vital to derive an analytical model, by means of which it is also possible to evaluate the effects of the variation of a single mechanical parameter, like the camera case inertia (e.g. due to a bird or to a change in the zooming level) or the support stiffness.

In Fig. 7 we report the multibody model of the camera positioning unit, w.r.t. the pan angle θ_2 motion. The left

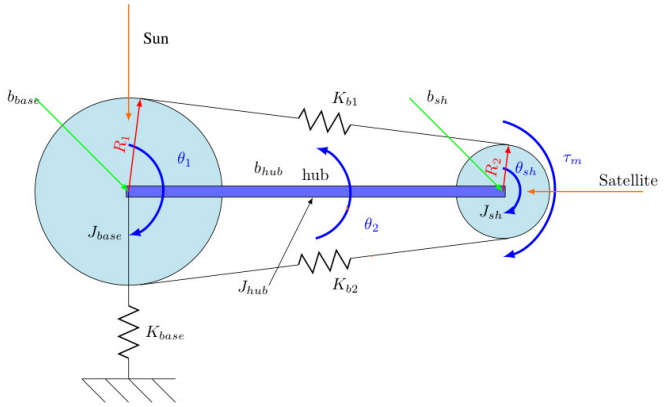

Fig. 7. Multibody model of the camera positioner.

part of the model is the fixed part of the unit (Sun), anchored to the ground through an elastic connection K_{base}; the right part represents the HSM, with inertia J_{sh}. The two parts are connected via the springs K_{b1} and K_{b2}, accounting for the transmission belt elasticity.

Also, we indicate with θ_1 the relative angular displacement of the base w.r.t. the fixed structure, with θ_2 the hub rotation angle (output), with θ_{sh} the rotor field angle w.r.t. θ_2, and with θ_u the stator field angle w.r.t. θ_2 (input).

In order to get the full model of the system, we need to define the input torque, generated by the HSM, and driving the hub rotation. It is worth noticing that, using the microstepping technique, the stator field can be oriented with an arbitrary angle θ_u, by driving the stator windings with two current in quadrature, namely $i_1 = I\cos(\theta_u)$ and $i_2 = I\sin(\theta_u)$. In absence of a load torque, the rotor aligns its magnetic axis with the stator field (i.e. $\theta_u = \theta_{sh}$). When an external load is applied, this causes a displacement between rotor and stator flux, according to

$$\tau_m = K_T\, I\, \sin\left(\theta_u - \theta_{sh}\right) \tag{1}$$

This, in turn, can be linearized for small displacement, around the equilibrium, yielding

$$\tau_m \approx K_T\, I\, (\theta_u - \theta_{sh}) \tag{2}$$

Clearly, the above result shows that the HSM behaves like a spring, with an equivalent stiffness depending on the motor torque constant K_T and the level of the driving current I.

The next step is to derive the transfer function of the system by considering the stator flux angular position θ_u as the system input and the hub (camera) angle θ_2 as the system output. It can be proved that such transfer function has three pairs of complex conjugate poles and two pairs of complex conjugate zeros:

$$\frac{\Theta_2(s)}{\Theta_u(s)} = \frac{(s^2 + 2\xi_{z1}w_{z1}s + w_{z1}^2)}{(s^2 + 2\xi_{p1}w_{p1}s + w_{p1}^2)} \times \cdots$$
$$\cdots \times \frac{(s^2 + 2\xi_{z2}w_{z2}s + w_{z2}^2)}{(s^2 + 2\xi_{p2}w_{p2}s + w_{p2}^2)(s^2 + 2\xi_{p3}w_{p3}s + w_{p3}^2)}, \tag{3}$$

$\Theta_2(s)$ ($\Theta_u(s)$) being the Laplace transform of θ_2 (θ_u).

It is worth noticing that in all the above derivation, for the sake of simplicity, no difference between electrical and mechanical angle of the HSM motor has been explicitly shown, even if they have been considered in the derivation of (3). In practice, the motor used in the positioning unit has $N_r = 50$ teeth, corresponding to 1.8° of step angle. As for the ratio between motor and load position, it is $N_G = \theta_2/\theta_u = 1/7$.

We identified experimentally the frequency response of the actual system, by using both a sweep signal and a filtered white noise as a driving signal θ_u. Notably, the load position cannot be sensed directly, since this would require major (unwanted) modification to the hardware design and sensible component cost increase. Instead, we used a low–cost MEMS accelerometer, that can be easily placed on top of the camera case (see Fig. 8). Clearly, the measured tangential acceleration is proportional to the load angular acceleration $\ddot{\theta}_2$, from which it is possible to recover the angular position.

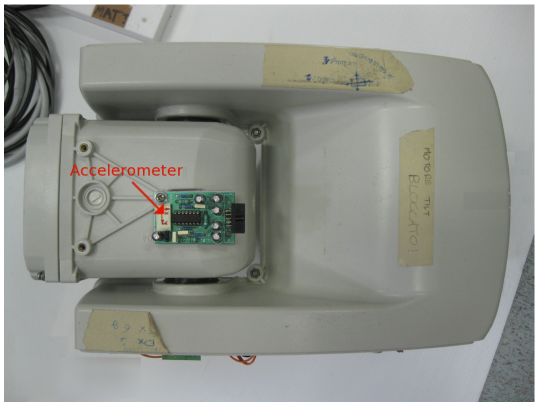

Fig. 8. MEMS accelerometer placed on top of the camera case.

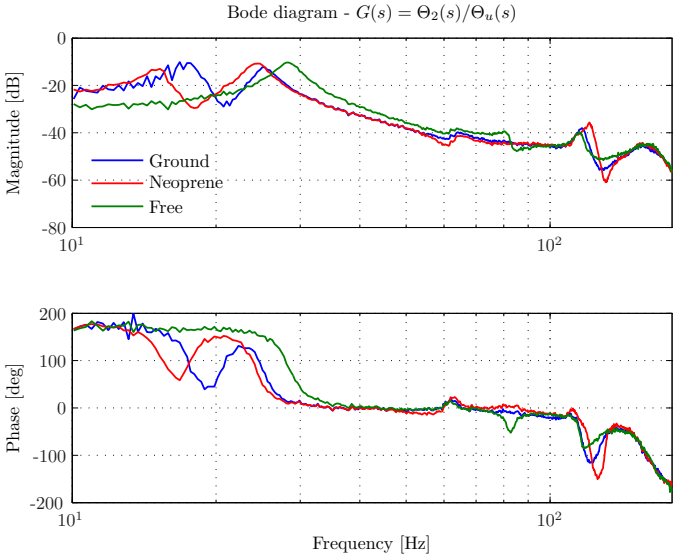

Fig. 9. Experimental frequency response $\Theta_2(s)/\Theta_u(s)$ with different support stiffnesses.

We report in Fig. 9 the frequency response obtained with spectral analysis methods and limited-bandwidth white noise excitation. Three different types of connection with floor are considered, namely with high, medium and zero stiffness K_{base} (the latter obtained by using a ball–bearing support). As an expected result, the pole-zero pair at low frequency disappears in case of zero stiffness, with a consequent order reduction in the plant to be controlled. Excluding the latter condition, being not realistic, we can observe that the system shows two evident resonance peaks, which can possibly amplify the torque ripple. With a concrete base, the resonant frequencies are 17.55 Hz and 25.95 Hz, respectively.

4. CONTROL LAW DESIGN

In order to design the active damping control, the experimental frequency response has been fitted into the analytical model whose structure is defined in (3). The Bode plot for nominal plant (concrete base and nominal camera inertia) is shown in Fig. 10. Note that the static gain corresponds to the gear ratio N_G.

The rationale behind the active damping strategy is to set up an inner loop, capable of reducing the height of

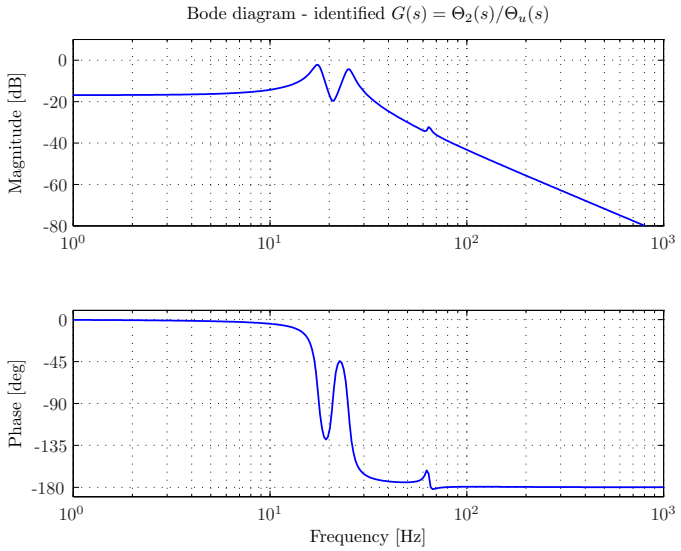

Fig. 10. Fitted Bode plot (by using a frequency-domain least-square fitting procedure) of $\Theta_2(s)/\Theta_u(s)$ in nominal conditions.

the resonant peaks as well as the oscillations that may be caused by various disturbances. In approaching the design of such inner control, we must take into account several constraints, due to the use of HSM and to the specific application under study. As for the latter, we must consider that there is no precise knowledge about the transfer function, since this may widely change during operation (e.g. when a bird lands on the camera, the load inertia increases and, in turn, all resonance frequencies decrease). Of course, an on-line identification procedure could be implemented (e.g. Wang and Tomizuka [2008]), but this is not compatible with the uninterruptible 24-7 operating scenario of the surveillance camera and the possible sudden and large variations in plant parameters. Then, a typical active damping scheme, with a feedback tuned on the plant resonances (see, for instance, Han et al. [2008]) cannot be applied to the camera positioning unit of interest. Given the above limitation, we resorted to a simple and robust solution, making use of a load velocity feedback, equivalent to inserting a viscous damper between load and base. This, in turn, is equivalent to commanding the actuator to generate a torque proportional to the load speed.

HSMs, however, are position actuators, so the question is: how to command HSM to generate a damping torque? The answer is handed by (2), which says that if we modulate the stator flux angle θ_u, we modulate the generated torque as well (this under the hypothesis of small differences between stator and rotor angles). Using this simple consideration, a vibration damping inner loop can be realized in the form shown in Fig. 11, where the load side velocity is obtained by integrating the load acceleration, measured using the MEMS accelerometer. Remarkably, the proposed method to generate a compensating torque in HSM–driven system can be applied also in systems with fixed plant parameters, for which more sophisticated damping schemes can be applied (Han et al. [2008]). In practice, if the target is going to be followed with a constant camera angular speed ω_t, this is achieved by setting the phase currents in the HSM as in (4)-(5), where θ_{ur} represents the desired

load position:

$$i_1 = I\cos(\theta_{ur}) = I\cos(\omega_{ur}t) = I\cos(N_r/N_G\,\omega_t\,t) \quad (4)$$

$$i_2 = I\sin(\theta_{ur}) = I\sin(\omega_{ur}t) = I\sin(N_r/N_G\,\omega_t\,t) \quad (5)$$

When the active damping inner loop is active, the actual angular position for the stator flux is obtained as follows

$$\theta_u = \theta_{ur} - K\,\dot{\theta}_2 \quad (6)$$

i.e. by subtracting a signal proportional to the load angular velocity to the reference angle θ_{ur}. This, as shown above, is equivalent to ask to the HSM to generate a torque proportional to the load angular velocity, as required by the active damping strategy. It is worth noticing that the actual implementation of the inner loop must take into account that the MEMS accelerometer may have some bias and high frequency noise in its output, so a band–pass filter must be placed in the feedback path of the control scheme in Fig. 11.

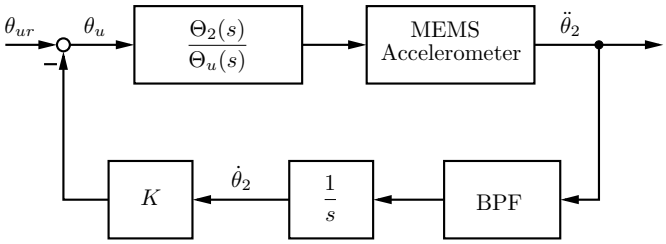

Fig. 11. Active damping inner loop.

The design of the inner loop clearly reduces to the choice of the feedback gain K. Actually, if the damping of the resonant modes is the control objective, a high value of K would lead to better results, as shown in Fig. 12.

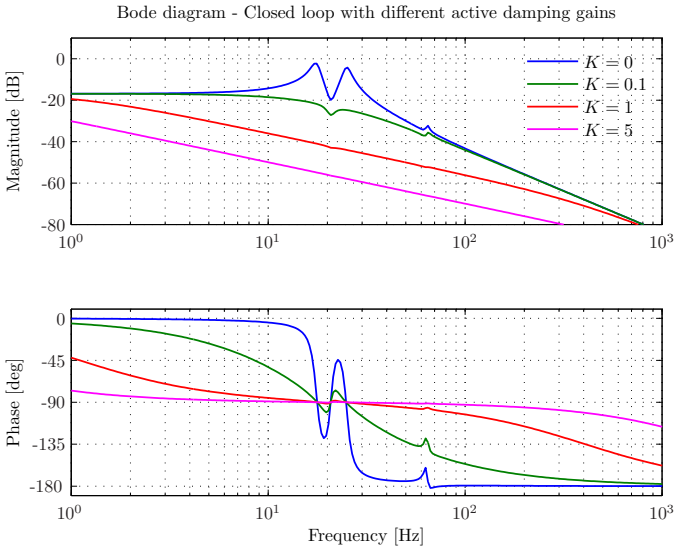

Fig. 12. Input/output frequency response with different compensation gains.

On the other hand, this choice leads to two problems. The first is that the amplitude of the compensation signal may become larger than a quarter of the HSM step width, and this may cause the rotor of the HSM to fail to follow the reference profile. The second problem is related to the promptness of the system. Typical reference positions have a ramp-like profile, and the steady-state error increases as the bandwidth of the system decreases. Fig. 13 shows the simulated time plot of the error (in [deg]) between reference and actual position in case of $K = 1$ and $K = 100$, respectively. It can be seen that with the second choice for the gain, the reference following error is rather large, so this choice would lead the actual camera position to lag behind the desired one, and, in turn, to loose the view of the moving target within the image plane. Then, the best choice for the compensation gain K has been done by considering the maximum slope for the motion commands (about $180°/s$) for the device considered.

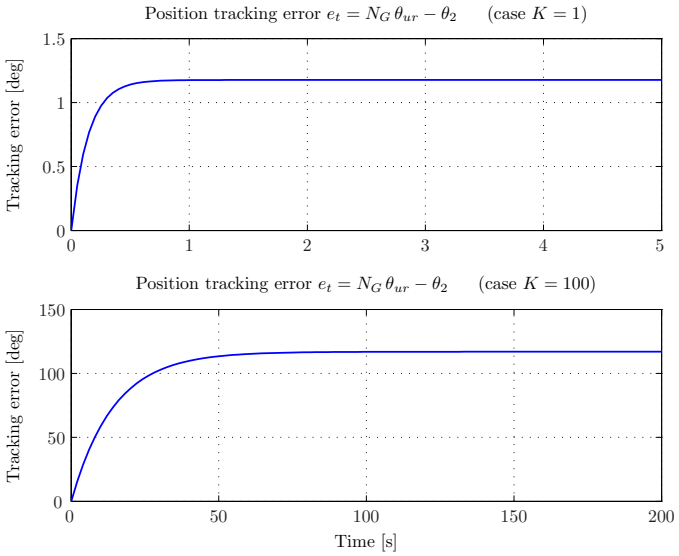

Fig. 13. Ramp reference following error (top plot: case $K = 1$; bottom plot: case $K = 100$)

5. EXPERIMENTAL RESULTS

The active damping control presented in the previous section has been applied to the camera positioning unit and its effectiveness proven in different operating conditions. Fig. 14 shows the comparison of the spectra of the accelerations measured by the MEMS accelerometer, with and without the active damping. The rotating speed is chosen so that the first harmonic of the torque ripple falls in the resonant peak of the frequency response. As a result, a reduction of 95% of the vibration amplitude is achieved.

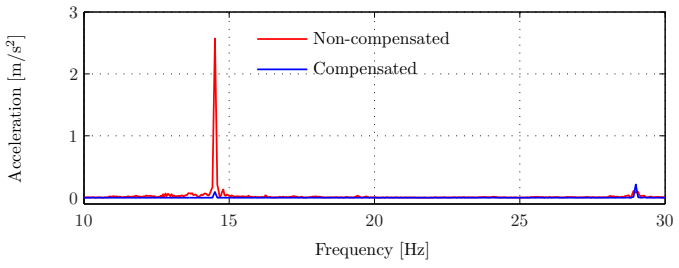

Fig. 14. Vibration attenuation at constant speed.

The same test at constant speed has been performed with different supports (with different rigidity), in order to test the insensitivity of the solution to the mounting conditions. Fig. 15 shows the results obtained with teflon and neoprene supports, confirming the robustness of the method.

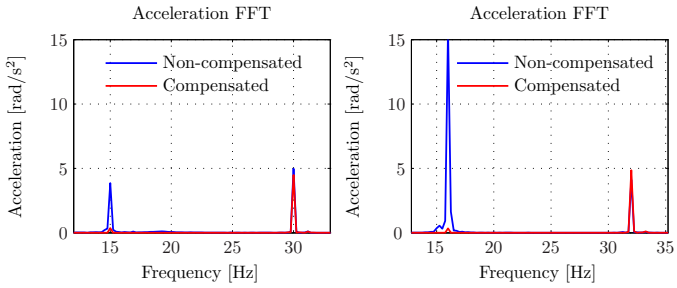

Fig. 15. Vibration attenuation with different supports (teflon on the right, neoprene on the left) – constant speed reference.

The robustness against support variations has been tested also in transient conditions (constant acceleration) and the results reported in Fig. 16 confirm the ability of the system to provide an effective damping of all vibratory modes.

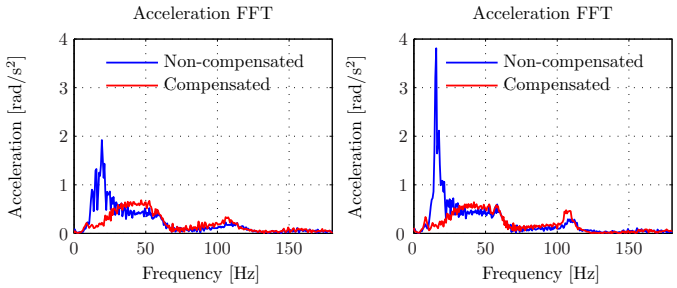

Fig. 16. Vibration attenuation with different supports (teflon on the right, neoprene on the left) – constant acceleration reference.

Finally, the robustness against load inertia variations has been verified, by placing ad additional weight on top of the camera. The results shown in Fig. 17 confirm again the insensitivity of the proposed method to wide changes in operating conditions.

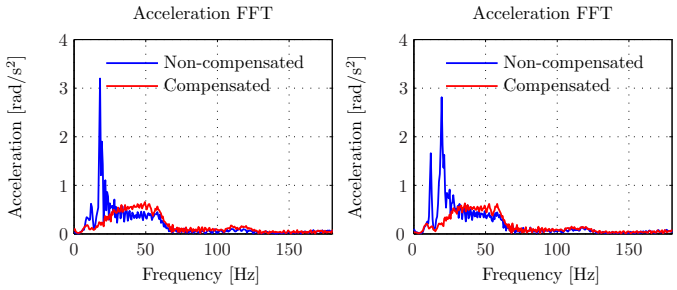

Fig. 17. Vibration attenuation with different load inertia (nominal on the left, doubled on the right) – constant acceleration reference.

6. CONCLUSIONS

Active damping control is widely adopted for reducing the vibrations in motion control systems. This technique, however, has been used so far only in those systems provided with a torque-controlled actuator. The reported application shows how it is possible to extend the application of this method even to motion control systems driven by HSM. The proposed solution can be easily retrofitted on existing hardware, being based on the use of load-side MEMS accelerometers and a simple modification of the microstepping technique. Experimental results show the robustness and effectiveness of a simple load velocity feedback in suppressing vibrations. The method developed for driving the HSM in order to produce a compensation torque can be applied to other mechatronic systems and its use in conjunction with more complex control schemes, possibly adaptive, will be the subject of future research.

ACKNOWLEDGEMENTS

Authors will like to thank Videotec (Schio, Vicenza, Italy) for providing (and allowing to hack) the camera positioning unit. Thanks also to Andrea Parisotto, Daniele Pellizzer, Marco Peruzzo and Mattia Schiesaro for their valuable contribution to the experimental activity.

REFERENCES

Hyo-Sung Ahn, YangQuan Chen, and Huifang Dou. State-periodic adaptive compensation of cogging and Coulomb friction in permanent magnet linear motors. In *American Control Conference, 2005. Proceedings of the 2005*, pages 3036 – 3041 vol. 5, jun. 2005.

L. Bascetta, P. Rocco, and G. Magnani. Force ripple compensation in linear motors based on closed-loop position-dependent identification. *Mechatronics, IEEE/ASME Transactions on*, 15(3):349 –359, jun. 2010.

A.J. Blauch, M. Bodson, and J. Chiasson. High-speed parameter estimation of stepper motors. *Control Systems Technology, IEEE Transactions on*, 1(4):270 –279, dec. 1993.

M. Bodson, J.N. Chiasson, R.T. Novotnak, and R.B. Rekowski. High-performance nonlinear feedback control of a permanent magnet stepper motor. *Control Systems Technology, IEEE Transactions on*, 1(1):5 –14, mar. 1993.

Cheng-Huei Han, Chun-Chih Wang, and M. Tomizuka. Suppression of vibration due to transmission error of harmonic drives using peak filter with acceleration feedback. In *Advanced Motion Control, 2008. AMC '08. 10th IEEE International Workshop on*, pages 182 –187, mar. 2008. doi: 10.1109/AMC.2008.4516063.

T. Kenjo. *Stepping Motors and Their Microprocessor Controls*. Clarendon Press, Oxford, 1984.

D. Kos, A. Kapun, M. Curkovic, and K. Jezernik. Efficient stepper motor torque ripple minimization based on fpga hardware implementation. In *IEEE Industrial Electronics, IECON 2006 - 32nd Annual Conference on*, pages 3916 –3921, nov. 2006.

J. E. McInroy, R. M. Lofthus, and S. A. Schweid. Step motor supply: Minimizing torque ripple induced by digital linearization. *Control Engineering Practice*, 3(9): 1225 – 1235, 1995.

D.K. Miu. *Mechatronics*. Springer Verlag, New York, 1993.

M.F. Rahman and C. Grantham. Design approaches for microstepping step motor controllers. In *Power Electronics and Variable-Speed Drives, 1991., Fourth International Conference on*, pages 253 –257, jul. 1990.

Chun-Chih Wang and M. Tomizuka. Sensor-based controller tuning of indirect drive trains. In *Advanced Motion Control, 2008. AMC '08. 10th IEEE International Workshop on*, pages 188 –193, mar. 2008.